

CONFINEMENT VELOCITY FOR SMOKE IN TUNNELS – HOW TO POKE A STICK AT IT

¹Michael Beyer, ^{1,2}Conrad Stacey

¹Stacey Agnew Pty Ltd, AU

²Delve Stacey Agnew LLC, US

DOI 10.3217/978-3-85125-996-4-43 (CC BY-NC 4.0)

This CC license does not apply to third party material and content noted otherwise.

ABSTRACT

In 2023, NFPA 502 changed from the absolute prevention of backlayering (critical velocity) to allowing some backlayering (confinement velocity). That made sense for tunnel safety. However, it is not clear how to design for that. NFPA 502 does not provide any guidance on how to determine such a confinement velocity and there is no reliable calculation method that can be used for real (full-scale) tunnels. The complexity of determining confinement velocity and the parameters that influence backlayering are explored. Those influences are quantified via a CFD model validated for critical velocity, also understanding the importance of parameters like wall roughness, wall temperature etc. Surprisingly, in some circumstances, confinement velocity is no less than critical velocity. Guidance on how to approach confinement velocity for real projects is also offered.

Keywords: Smoke control, smoke propagation, confinement velocity, critical velocity

1. INTRODUCTION

Strategies for smoke control during tunnel fires vary considerably. Different countries have different approaches through their national standards. One of the philosophies is to prevent smoke propagation upstream of the fire by achieving critical velocity. Other philosophies acknowledge the adverse effects of higher airspeeds on smoke layer mixing, fire growth rates and peak heat release rates (HRR), and apply a lower velocity, accepting some upstream propagation of a hot smoke layer. That can be specified as a fixed velocity that is lower than critical velocity (e.g. 1.0 to 2.0 m/s) or allowing smoke backlayering up to a fixed length (e.g. 30 m). The low velocity approach minimises the risk of adversely affecting the egress conditions during the self-rescue phase, but, depending on the actual fire scenario and tunnel parameters, the smoke layer can propagate upstream for distances of several metres up to a couple of hundred metres. The maximum allowable backlayer approach is a compromise between low velocity, with the risk of having ‘uncontrolled’ upstream propagation of a smoke layer, and achieving high velocities for an absolute prevention of upstream smoke propagation. A tunnel air velocity that confines upstream smoke propagation to a specific distance is termed a confinement velocity. A more comprehensive discussion on the different smoke management philosophies can be found in [1] and [2].

NFPA 502, the national standard in the US, historically proposed a ‘critical velocity’ approach, but with the 2023 edition [3], changed its terminology from preventing backlayering to controlling backlayering, and now refers to a confinement velocity. However, even if such an approach is desired, no guidance on how to achieve confinement velocity is offered in the standard. Also, the literature does not provide information that can reliably be used for design purposes. Full-scale fire tests are rare, expensive and usually designed for a particular purpose, where it is often not possible/reasonable to draw conclusions outside of the test purpose. The Memorial Tests [4], [5], [6], for example, were designed (among other purposes) for analysing critical velocity over a wide range of fire heat release rates. So, the focus was on identifying

the condition where the thermal force generated by the fire was balanced by the pressure force of the longitudinal airflow approaching the fire [4]. Beyond that point, no steady state backlayering length in combination with almost constant air velocity and fire heat release rate were explicitly documented in the test reports. Also, the instrument loops upstream of the fire beyond the first loop were too widely spaced to observe either the backlayering distance accurately or the steadiness of a backlayer.

Full-scale tests were also performed in the Koralmtunnel, again with fire pans, but with smaller fire heat release rates, up to 20 MW. The purpose of those tests was to analyse smoke ingress into cross passages with the focus on measuring temperature distribution and analysing smoke propagation downstream of the fire. Based on observations during the field tests, a smoke backlayering length for selected tests are documented with an uncertainty of several metres [7]. The stated backlayering length (in [7]) occurred just before reaching peak-HRR, with no indication whether either the smoke propagation or the HRR were stable at that time. Also, the upstream air velocity was not kept constant during the fire tests (as stated in [7]), and therefore a conclusion on confinement velocity (backlayering length vs. upstream air velocity) can't be made reliably.

There are numerous small-scale tests based on Froude scaling [8], [9], [10], [11], [12], [13], [14], [15] with the objective to analyse critical velocity and/or backlayering length for different fire settings. However, as discussed in [16] and [17], the Froude number widely used for Froude scaling misses the buoyancy term that is very important for the backlayering flow regime. There is no evidence that the data produced in small-scale tunnels can be scaled up to a real tunnel by any parameter, and therefore it is unclear if the flow regime established in the small-scale tunnels represents the situation in a real tunnel. Any proposed equation for calculating a backlayering length, confinement velocity, or critical velocity derived from such small-scale tests needs to account for all relevant physics before it could be considered for use for real tunnels. To date, attempts to find non-dimensional relations to allow appropriate scaling of the relevant physics have fallen short.

As discussed above, there is not much guidance available on how to approach confinement velocity for fires in real tunnels. So, as designers, how do we poke a stick at it?

Beyer, Stacey & Brenn [17] recently proposed a mixed convection model for estimating critical velocity for smoke control in road tunnels. As the flow regimes relevant to critical velocity and confinement velocity are expected to be very similar, the important aspects that influence critical velocity according to [17] will likely also influence the confinement velocity. Before addressing confinement velocity, the main findings on critical velocity provided by [17] will be summarised.

2. CHARACTERISTICS OF FLOW REGIME

When achieving critical velocity or confinement velocity, the buoyancy force relevant for developing a backlayer of hot smoke is in the order of the inertial force relevant for pushing the smoke downstream. Such a flow regime can be defined as mixed convection and characterised by the Richardson number $Ri = Gr/Re^2$ (strength ratio between natural convection and forced convection). Interestingly, a similar definition of the Richardson number is sometimes quoted as ‘critical Froude number’ in the tunnel community and fire engineering field [18], [19], [20]. However, it is important to note that the ‘critical Froude number’ is very different to the Froude number behind the so-called Froude-scaling of such flows. The number that has been used for scaling represents the ratio of the inertial force to the gravity force and neglects the buoyancy term. Froude number is central for any isothermal fluid flow which can be significantly influenced by the body force due to gravity (e.g. water

waves in open channel flows), but it does not characterise buoyancy driven flows and therefore should not have been used for scaling attempts [16], [17].

In the Richardson number, the Grashof number Gr is a measure of the natural convection and the Reynolds number Re a measure of the forced convection. Using the tunnel hydraulic diameter D_h as the relevant length scale for the forced convection and the tunnel height from the fire base L_n as relevant for the natural convection, the velocity relevant for upstream smoke propagation U can be expressed [17] as:

$$U = K_F K_g \left(\frac{g L_n^3}{D_h^2} \frac{1}{Ri} \frac{\Delta T}{T_a + \Delta T} \right)^{1/2} \quad (1)$$

The temperature T_a refers to the ambient temperature of the approaching air. Appropriate definition of the parameters K_F , K_g , Ri and ΔT for estimating critical velocity will be summarised in the following section. For a more comprehensive discussion refer to [17].

3. CRITICAL VELOCITY

The following section provides a short summary of the physical model for estimating critical velocity as presented in [17]. The intention here is to discuss the essential parameters that influence critical velocity as they will also be relevant for the even more complex flow regime around confinement velocity.

For critical velocity it is assumed that the strength of forced convection is of the same order as the strength of natural convection, which requires that the Richardson number in equation (1) is unity.

One of the challenges is, to identify an appropriate temperature difference ΔT relevant for the buoyancy term. As discussed in [17], the first aspect that is important for estimating the effective temperature difference is the fire intensity (heat release rate per unit area). The more heat that gets released per unit area, the higher is the density deficit and thus the buoyancy force. That is, the relevant buoyancy force for establishing a backlayering is not necessarily a function of the fire heat release rate. This was also observed during the Memorial Tunnel tests where the fire heat release was increased by adding fire pans (same fire intensity) in the longitudinal direction with the result that the observed critical velocity value was essentially unchanged between 20 MW and 100 MW [4]. The second important aspect is how much of the front bit of the fire contributes to the buoyancy force relevant for creating a backlayer. When increasing the fire heat release rate by extending the fire in the longitudinal direction but keeping the fire width and fire intensity the same, the contribution of the downstream bit of the fire to the density deficit at the front of the fire becomes less important the longer the fire gets. According to [17], the contribution of the fire front in the effective temperature difference ΔT was found to be a function of the ratio between fire length and the length scale relevant for natural convection.

The mixing of the approaching air with the hot plume gases is the final important factor that influences the effective temperature difference. In [17] it is acknowledged that some of the approaching air passes the fire front without interacting with the hot plume. With a smaller plume frontal area, the hot plume gases are mixed with less of the approaching ambient air and the initial smoke layer temperature is reduced less. Along with the fire width influence below, this addresses the aspect ratio correction that was seen to be required on all methods that evaluated temperature rise using the total flow.

The influence of the plume frontal area on the approaching flow is another effect of the width scales of the fire and the tunnel, also detailed in [17]. If the plume frontal area is small compared to the tunnel area (wide tunnels), a bigger fraction of the flow avoids the rising

plume, with the plume less affected by the air slipping easily around it. For a wider fire with a plume area nearly as big as the tunnel area, a higher fraction of the flow momentum is ‘opposing’ the plume so that the velocity required to prevent backlayering goes down. The influence of the plume width on critical velocity in [17] was found to be a function of the ‘free area’ around the plume and is considered by the factor K_F in equation (1).

The final interesting outcome in the study provided in [17] is that the influence of the tunnel grade on the critical velocity can be neglected for tunnels with typical gradients ($\pm 6\%$). That is, the grade factor K_g in equation (1) becomes unity. When critical velocity is achieved and backlayering prevented, the gravity vector in the Grashof number that is relevant for the natural convection stays nearly the same for small tunnel slopes and so it is plausible that the critical velocity is not influenced by typical tunnel slopes. However, while a typical tunnel slope does not influence the critical velocity, it still has huge implications in the required ventilation power to achieve/maintain the required critical velocity, due to the buoyancy effects related to the hot smoke gases downstream of the fire.

With considering the essential effects on the relevant temperature difference for the buoyancy force and the influence of the fire width, together with the conclusion on the grade factor, the physical model for estimating critical velocity as proposed in [17] is able to predict critical velocity values for the relevant full-scale test as well as the measured dimensional values in small scale tunnels, all within an acceptable accuracy. As the physics relevant for upstream smoke propagation for fires in tunnels seems to be adequately captured with those equations, it appears to be an appropriate starting point for discussing confinement velocity.

4. CONFINEMENT VELOCITY

4.1. Influence on Local Fire Plume Dynamics

For confinement velocity (lower than critical velocity) the inertial force reduces relative to the buoyancy force so that the two forces are not in the critical velocity equilibrium, and hot smoke starts propagating upstream. This refers to a Richardson numbers >1 in equation (1). It is pretty straightforward how a change in the velocity upstream of the fire changes the inertial force, but it is difficult to estimate what it does to the effective temperature difference relevant for the buoyancy force ΔT and the fire width dependency as discussed in Section 3. We explore this a bit further.

The fire intensity influence on ΔT will be similar to the ‘critical’ case, but as smoke starts propagating upstream more of the fire length may contribute to the plume front that influences the buoyancy force. That potentially requires an adjustment of the relevant empirical parameters derived in [17]. The backlayering restricts the free flow area upstream of the fire, and potentially lowers the height at which the plume enters the smoke layer. That reduces the fraction of the fresh air mass flow that mixes with the plume, likely causing a higher ΔT . However, as the backlayering restricts the area for the approaching flow, there is less space for the air to get around the plume and that seems likely to cause a higher deflection of the plume (higher momentum onto the plume front) and more mixing into the plume (relative to the free upstream velocity). Consequently, the factor K_F might increase or stay the same. Both effects (plume front area definition for mixing and plume deflection) of course depend on the thickness of the backlayering (e.g. frontal area of the backlayering versus tunnel area) and potentially offset each other. Based on that rationale, it seems likely that the buoyancy force stays more or less the same between critical velocity and confinement velocity if the backlayering is stable and the length is limited (e.g. 20 to 50 m). Figure 1 and Figure 2 compare the temperature and velocity distributions resulting from a simulation of a 50 MW pool fire at some confinement velocity, and without upstream smoke propagation (critical velocity).

Any differences in the relevant/effective buoyancy force between critical velocity and confinement velocity for small backlayering distances could be tied into a modified Richardson number $Ri_B = Ri \cdot f_B$ required for restricting backlayering. According to equation (1) that would lead to following relation of confinement velocity U_B .

$$U_B = K_F K_g \left(\frac{gL_n^3}{D_h^2} \frac{1}{Ri_B} \frac{\Delta T}{T_a + \Delta T} \right)^{1/2} \quad (2)$$

4.2. Influence on Backlayer Dynamics

Equation (2) above may describe the initial momentum of the backlayering once backlayering starts to grow due to the imbalance of buoyancy and inertia force, but it does not address the physics relevant for the resulting backlayering length based on that imbalance. As an example, for the same tunnel air velocity (< critical velocity), the backlayering extent for a very rough tunnel wall will be lower than the backlayering extent for a very smooth tunnel wall. So, wall roughness likely is important as it reduces the resulting momentum of the backlayer, applying a retarding shear on the layer to supplement the shear from the flow underneath the layer. There are other effects related to heat transfer, thermal radiation, shear layer between the backlayering and approaching flow and tunnel slope that influence the resulting momentum and propagation of the backlayer. The heat transfer between the backlayering and the cooler tunnel wall, the thermal radiation between the underside of the backlayering and the cooler surroundings, and the mixing within the shear layer, all reduce the temperature of the hot smoke layer while moving upstream. That temperature reduction, as well as the interaction with the approaching air in the shear layer, reduces the resulting momentum of the backlayering and thus the upstream propagation of the hot smoke. The effect of the heat loss due to thermal radiation is assumed to be minor. Part of the cooler smoke in the shear layer flows against the backlayering and back to the fire front. That counterflow insulates the hot smoke layer adjacent to the tunnel ceiling and reduces heat loss by thermal radiation. If the tunnel is sloped, the gravity component in the longitudinal direction would have an additional effect on the resulting momentum of the backlayering due to the buoyancy force, and likely on the shear layer. Even if a typical tunnel slope does not affect critical velocity [17], it intuitively seems likely to affect the propagation of the backlayering.

The upstream smoke propagation stops, and is perhaps stable, once all the effects are in equilibrium. However, the backlayering may still slowly creep upstream while the tunnel wall adjacent to the backlayering gets hotter over time and so slowly reduces the heat transfer from the backlayer into the tunnel wall. A first estimation of the time-dependent temperature rise in the tunnel lining based on a one-dimensional transient heat transfer calculation (see Figure 9) shows that the wall heat flux adjacent to the backlayering decreases by 15% after 10 minutes, by 20% after 20 minutes and by 40% after 120 minutes. That suggests that the wall heat flux in the first 20 minutes reduces as much as in the following 100 minutes. With an important timescale of 20 minutes, there is only a slim chance of wall heating being important to egress. Tunnel shape and profile is a further aspect that likely influences the backlayer thickness and propagation (e.g. curved ceiling vs. flat ceiling, or horseshoe profile vs. rectangular profile with lower air velocity at the corners).

All of the above would be required to be appropriately implemented in a physical model, and possibly incorporated into equation (2), to be able to estimate a backlayering distance. In a further step, the empirical model would need to be adequately validated against a systematic parameter study or preferably, against full-scale test data. However, while full-scale test data are preferred, it will be very difficult to achieve a steady flow field with a backlayer of any significant length.

4.3. CFD study

To explore the influences on the propagation of the backlayering a bit further, a CFD model was created based on the proposed methodology used for evaluating critical velocity by Beyer & Stacey [21]. The overall methodology, mesh type and resolution as well as boundary conditions were kept the same. The simulation software ANSYS Fluent [22], [23], [24, 25] was used. The modelled tunnel has a typical 3-lane TBM profile with a cross section area of 93 m² with a hydraulic diameter of 9.9 m and a height from floor to ceiling of 8.92 m. The tunnel domain has a total length of 500 m. The fire source was placed 300 m downstream of the inlet portal on the floor in the middle of the tunnel. Adopted design fire parameters as proposed in [17] for a 50 MW fire, and other input parameters, are listed in Table 1.

Table 1. Input parameters used for the CFD model.

Parameter	Value
Tunnel air temperature	30°C
Wall temperature (constant)	30°C
Wall roughness height Ks	0.0015 m
Tunnel slope	Flat (0%)
Total Fire HRR	50 MW
Radiative fraction	0.2
Fire width	2.5 m
Fire intensity	2.25 MW/m ²
Fire length	8.889 m
Fuel	Fuel-oil (C ₁₉ H ₃₀)
Combustion efficiency based on total HRR (relevant for additional CO ₂ and H ₂ O source)	0.95

Based on the initial CFD model as described above, the critical velocity (no backlayer) and the confinement velocity for a backlayer length of 30 m was analysed to understand the variation in velocity between the two conditions.

In a further step, the influence of the tunnel slope, wall roughness and wall heating on the backlayer length were analysed. In all simulations, the confinement velocity (that was necessary in the base case to maintain the backlayer distance to 30 m) was kept the same and the variation in backlayering length compared to the base case CFD model. For the tunnel slope sensitivity, the results of the flat tunnel were compared to tunnels with 4% and 8% downgrade. The wall roughness influence was analysed by increasing the wall roughness height by a factor of 5, and also by simulating a smooth wall. Regarding wall heating, the initial simulation with a constant wall temperature (equal to approaching air temperature) was compared to a simulation where the wall temperature was increased in the upstream region where the smoke layer interacts with the tunnel wall. The wall temperature in the remaining upstream section and downstream of the fire front (between front of the fire and exit portal) was kept constant, as before. The wall temperature was estimated based on a one-dimensional transient heat transfer calculation (see Figure 9). Appropriate values for smoke temperature adjacent to the wall, and a heat transfer coefficient within the smoke affected region upstream of the fire were evaluated based on the initial simulation (30 m smoke backlayer). The surface wall temperature after 60 minutes resulting from the one-dimensional calculations was used as the wall boundary condition for the simulation with the heated wall. The comparison of the

simulations should provide information about the variation on backlayering length due to the wall heating effect for a fire that lasts approximately 60 minutes.

In a final step, critical and confinement velocities for a train fire in a rail tunnel with 3% downgrade were analysed. The train has a frontal area of approximately 8.4 m² and was stationary in the tunnel. The head of the train is positioned 300 m downstream of the entry portal. The fire source (1.8 m wide and 22 m long) is sitting on the floor of the second carriage and has a total HRR of 15 MW. As a “worst case” scenario (less train blockage and smoke/heat can more easily escape the carriage), it is assumed that the glass of all the windows was broken and that the doors at one side of the fire carriage were opened. The TBM tunnel profile has a free flow area of approximately 27.2 m², a hydraulic diameter of approximately 3.9 m and a total height of 5.4 m. The floor of the carriage is 1.13 m off the tunnel floor. With those parameters, the average annular velocity over the train is 1.446 times the average upstream velocity. The train wall was assumed to be adiabatic with a wall roughness height of 0.25 mm. Also, the walls of the installations (e.g. cable trays) were assumed to be adiabatic. The tunnel wall was simulated with a constant temperature of 21.4°C (same as ambient upstream air temperature) and a wall roughness height of 1.5 mm. All other input parameters and simulation settings were according to Table 1 and [21].

4.3.1. Results of the CFD Study

Critical velocity versus confinement velocity: The established critical velocity in the first simulation was slowly reduced until a steady state backlayering distance of 30 m was established. For the assessed tunnel and fire parameters, the critical velocity and confinement velocity are 3.54 m/s and 3.28 m/s respectively. Figure 1 and Figure 2 compare the temperature and velocity distributions at critical and confinement velocities. As discussed in Section 4.1, the comparison of the temperature field around the fire confirms that the plume shape and temperature distribution is very similar between critical and (30 m) confinement velocity. In the critical velocity simulation, the fire is spread downstream a bit more, as the velocity onto the flame front is slightly higher (see Figure 2) compared to the case with confinement velocity. Also, the temperature at the upper part of the plume close to the ceiling is slightly higher with the lower confinement velocity airspeed.

Figure 2 indicates that while the average upstream velocity in the case of a 30 m backlayer is less than critical velocity, the velocity under the smoke layer and onto the fire is nearly as high as for the critical velocity case. This of course is related to the smoke layer thickness reducing the free area for the upstream flow. Figure 3 illustrates the temperature profile for the case with smoke backlayering, and the velocity profile for both cases (50 MW in a flat tunnel). The temperature profile provides information on the shear layer thickness (approximately 2.5 m in this case) and the velocity profile gives information on the velocity gradient in the shear layer (from -1.5 m/s to 4.2 m/s in this case). It is interesting to see that, below the smoke layer, the approaching velocity at the front of the fire pans for the lower confinement velocity case is higher than for the critical velocity case. However, while hard to see in Figure 2, the velocity onto the flame front is still slightly higher with critical velocity.

When assuming that the overall fire plume dynamics can still be described by equation (1) (Ri at critical velocity is 1.0) the modified Richardson number Ri_B required for maintaining a backlayer distance of 30 m would be 1.25 according to equation (2) ($U_B = U_c / \sqrt{Ri_B}$). That implies that the model assumptions (e.g. tunnel profile, wall roughness, tunnel slope, wall temperature etc.) and the subsequent influences on the backlayer and fire plume dynamics are included in the modified Richardson number. Any difference in the model assumptions would either result in a different backlayer distance (if a steady state layer still arises) or in a different modified Richardson number to achieve the same backlayer distance of 30 m.

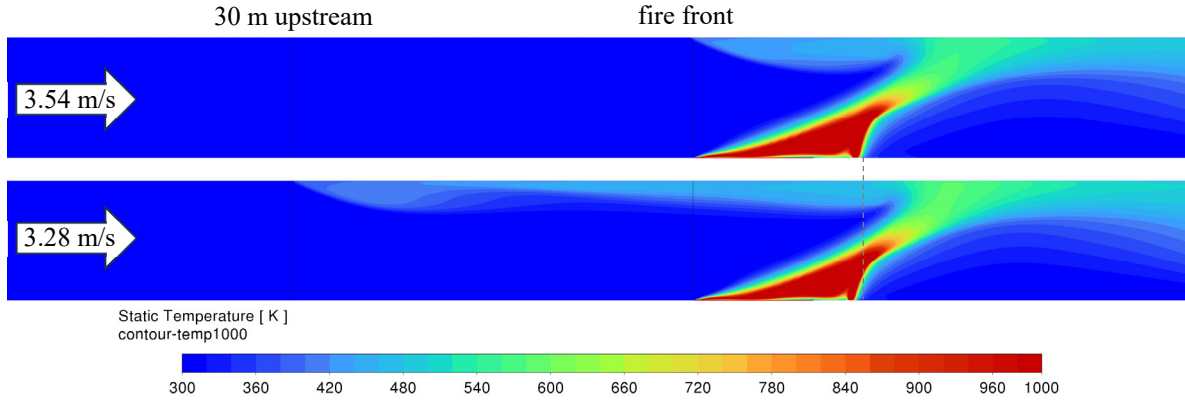


Figure 1: Contour plot of temperature distribution through the middle of the tunnel for critical velocity (top) and confinement velocity (bottom) – Initial CFD model. Temperature is clipped to 1000 K for better presentation.

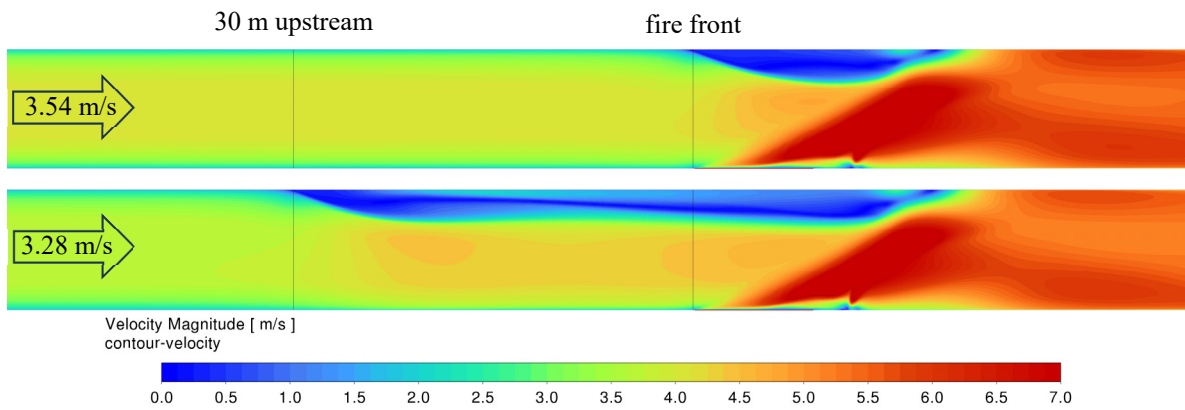


Figure 2: Contour plot of velocity distribution through the middle of the tunnel for critical velocity (top) and confinement velocity (bottom) – Initial CFD model. Velocity is clipped to 7 m/s for better presentation.

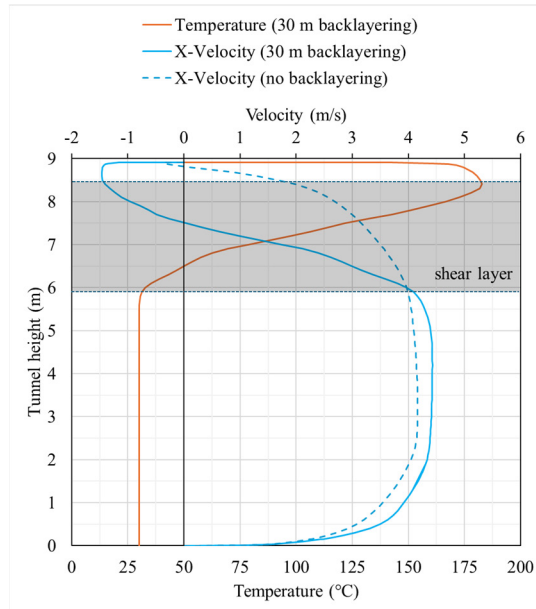


Figure 3: Velocity and temperature profile at the fire front for confinement velocity, and velocity profile for critical velocity. The profiles were taken on a vertical line from tunnel floor to ceiling in the symmetry plane of the tunnel profile.

Tunnel slope influence: To explore the slope influence on the upstream smoke propagation, the initial simulation with confinement velocity in a flat tunnel was repeated for a 4% and 8% downgrade. All the other parameters were kept the same, including the oncoming airspeed. The results at 4% downgrade were surprising. Instead of getting the expected increase in smoke backlayering distance, the smoke backlayer length was reduced by approximately 50% and oscillated between 10 m and 15 m. The simulation with the 8% downgrade tunnel showed a similar outcome. Figure 4 compares the temperature distribution in the flat tunnel with that in the sloped tunnel (4% downgrade) and depicts the amplitude of the smoke layer oscillation (transient behaviour) observed in the sloped tunnel. Temperature and velocity distribution for the tunnel with the 8% downgrade are shown in Figure 5, at nearly the maximum extent of the smoke advance, before the smoke backlayer moved backwards again. Based on that flow field, the velocity and temperature profile at the fire front were compared in Figure 6 to the profiles obtained for the flat tunnel (according to Figure 3). Examination of the flow field and the profiles confirmed that the additional buoyancy force in the smoke backlayer increases the velocity in the backlayer. That results in more smoke volume propagating upstream (higher smoke mass flow), creating a thicker smoke backlayer. The higher speed and the thicker backlayer increase the shear layer and the shear stress onto the backlayer (relative velocity between smoke backlayer and approaching air). That also seems to create instability in the flow, which of course increases mixing. It may be a moot point whether the extra shear or the instability cause the effect seen, as they are causally linked, but the effect is clear; that the smoke layer can’t propagate further upstream. In the unstable behaviour, the smoke layer increases in thickness and finally gets caught by the approaching air, mixed down and pushed back towards the fire, before it starts over again. While the smoke layer increases in thickness, the velocity onto the fire increases as well so that the fire plume behaviour and the generated buoyancy force likely change in favour of pushing the smoke layer back (assisting the oscillation). Figure 6 shows that the peak velocity of the smoke propagating upstream in the tunnel with 8% downgrade is almost twice as high as in the flat tunnel. Also, the smoke layer thickness increases by approximately 1 m. Despite these factors that would be expected to increase the backlayering length, the backlayer is much smaller.

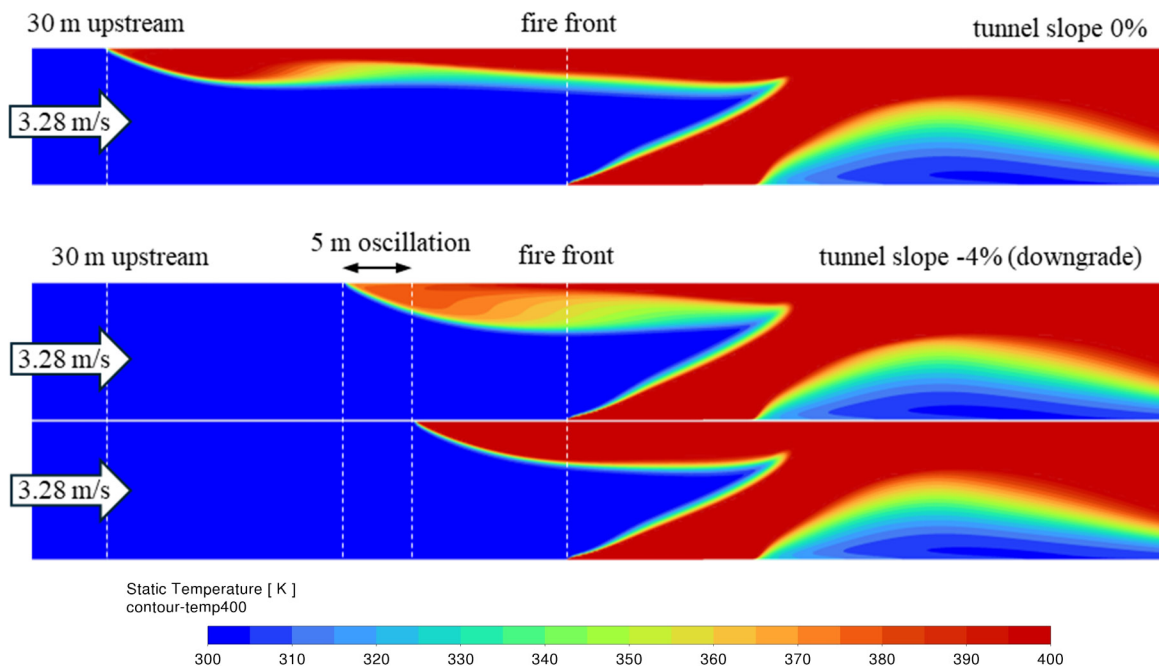


Figure 4: Contour plot of temperature distribution through the middle of the tunnel for confinement velocity in a flat tunnel (top) and a tunnel with 4% downgrade (bottom). The comparison in the bottom picture indicates the amplitude of the smoke backlayer oscillation. Temperature is clipped to 400 K for better presentation.

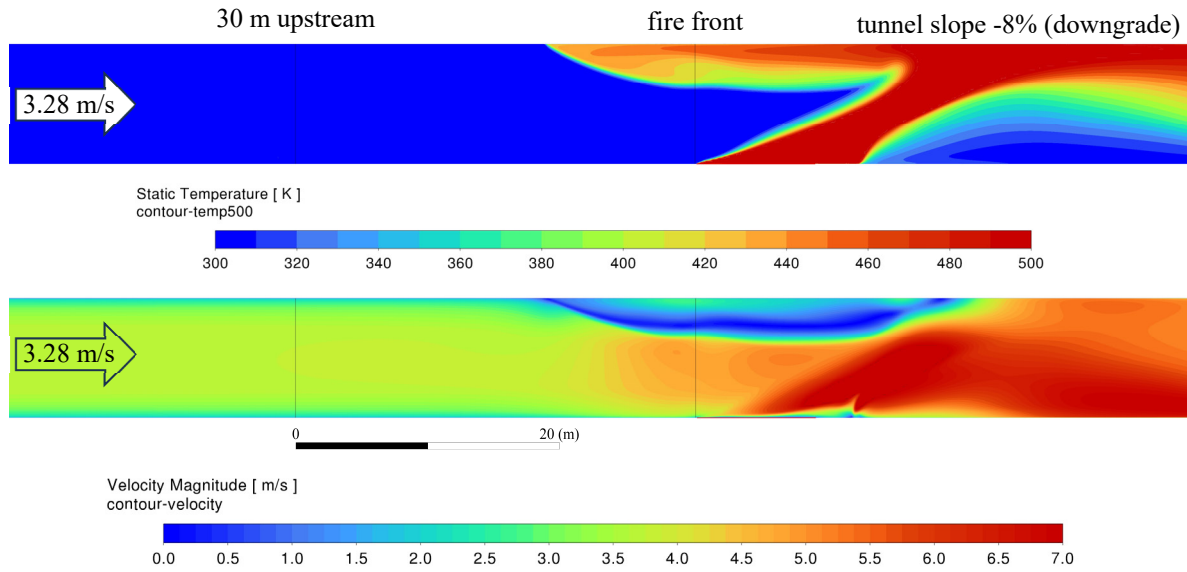


Figure 5: Contour plot of temperature (top) and velocity distribution (bottom) through the middle of the tunnel for confinement velocity and a tunnel with 8% downgrade. Temperature is clipped to 500 K and velocity is clipped to 7 m/s for better presentation.

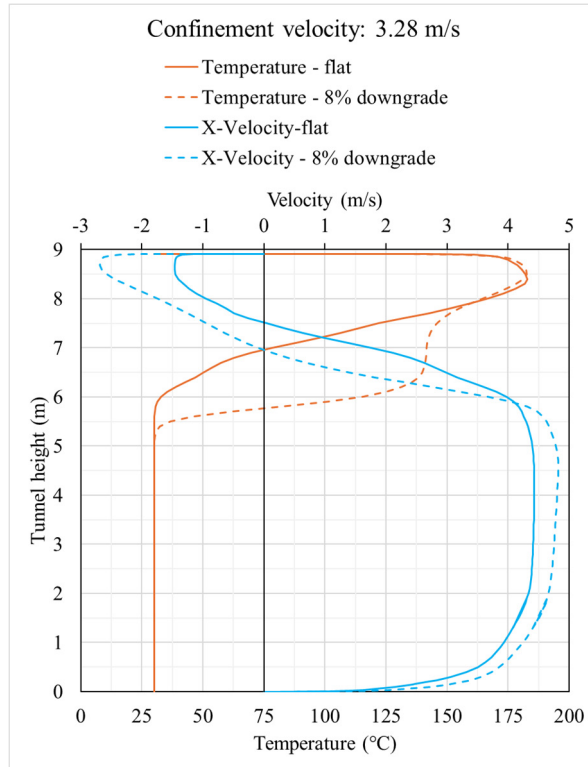


Figure 6: Velocity and temperature profile at the fire front for confinement velocity in a flat tunnel and a tunnel with 8% downgrade. Profile was created on a vertical line from tunnel floor to ceiling in the symmetry plane of the tunnel profile.

Wall heating influence: The wall temperature adjacent to the smoke backlayer was estimated based on a one-dimensional transient heat transfer calculation (results are shown in Figure 9). According to the initial simulation with confinement velocity (backlayer distance of 30 m) the smoke temperature adjacent to the wall and the heat transfer coefficient in the upstream smoke layer were evaluated to be 367 K and 10.3 W/m²K respectively. These values were used as boundary conditions for the one-dimensional transient heat transfer calculation. The estimated wall surface temperature after 60 minutes of 324 K (increase of approximately 21°C) was used as a wall boundary condition in the smoke affected region upstream of the fire, and the simulation repeated. As indicated in Figure 7, the backlayer distance increased from 30 m to 35.4 m (18%) within 60 minutes, due to the wall heating. Figure 8 compares the velocity and

temperature profile at the fire front and shows that the initial velocity and temperature distribution of the upstream smoke layer stays almost the same. That indicates that the initial momentum of the smoke layer decays slightly less with less wall heat transfer when propagating upstream. The increase in backlayering length by 18% for a fire duration of 60 minutes might be acceptable and therefore wall heating may not be an essential inclusion in calculations for estimating confinement velocity. That assumes that the accepted backlayer length is in the range assessed here. The influence on a backlayer distance much higher than 30 m may have a bigger impact on the extra length due to wall heating and so wall heating may then become essential.

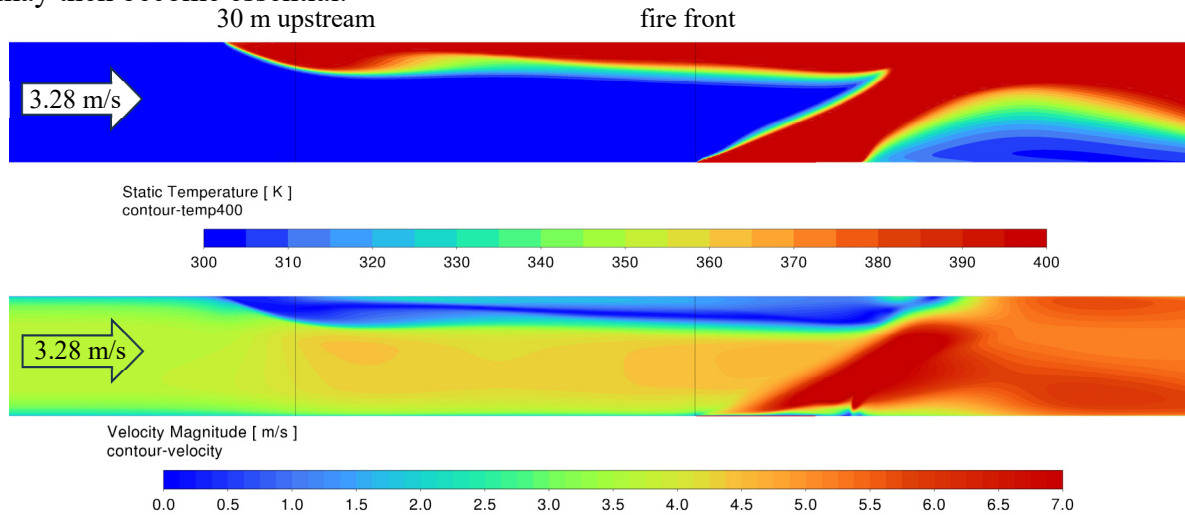


Figure 7: Contour plot of temperature (top) and velocity distribution (bottom) through the middle of the tunnel for confinement velocity with heated wall (heated wall for fire duration of 60 minutes) in the smoke affected wall region upstream of the fire. Temperature is clipped to 400 K and velocity is clipped to 7 m/s for better presentation.

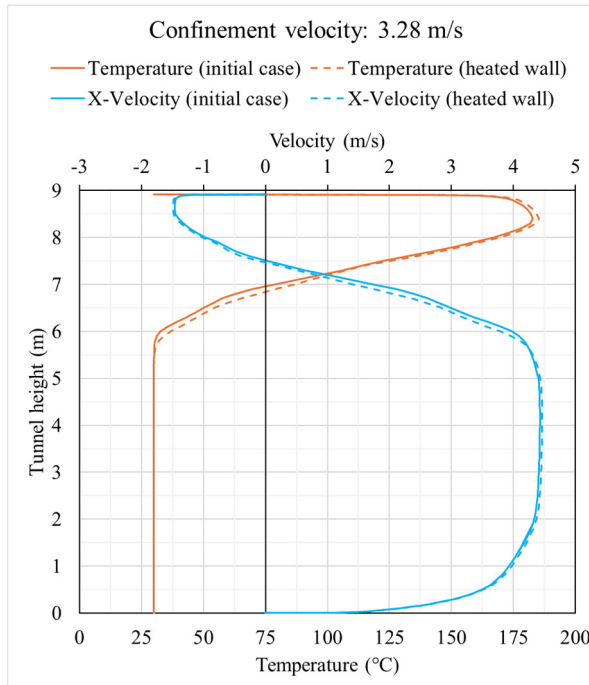


Figure 8: Velocity and temperature profile at the fire front for confinement velocity with constant wall temperature and increased wall temperature (heated wall for fire duration of 60 minutes). Profile was created on a vertical line from tunnel floor to ceiling in the symmetry plane of the tunnel profile.

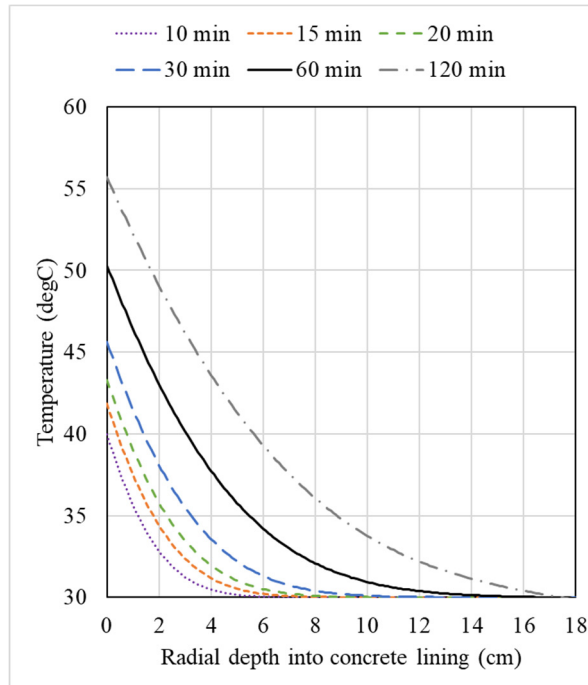


Figure 9: Temperature distribution in concrete lining over time. The radial depth of 0 cm refers to the smoke adjacent wall surface with an inner radius of 4.96 m. Calculations are based on one-dimensional (radial) transient heat transfer.

Wall friction influence: Based on the initial simulation, the typical wall roughness height of $K_s = 0.0015$ m, was increased by a factor of 5 to $K_s = 0.0075$ m and the simulation repeated. A further simulation with smooth wall was also conducted. All other parameters were kept the same. Figure 10 depicts the temperature and velocity distributions of the steady state backlayering with both the increased wall roughness and a smooth wall. With the rougher wall, the backlayer went back from an initial 30 m to a length of 7.8 m (reduction of 75%). For a smooth wall, backlayer length increased by 5.7 m (increase of 19%). Interestingly, the relative reduction in backlayer length for the rougher wall is almost as much as the wall roughness increase. The maximum upstream velocity in the smoke layer at the fire front was reduced by 20% due to the much higher wall roughness (Figure 11) and slightly increased for the smooth wall condition. When considering that a wall roughness height of 0.003 m [26] already refers to a very rough concrete surface, the simulation results likely show the maximum variation in backlayer distance related to wall roughness for any usual concrete tunnel wall. Of course, high effective roughness can also be created by fittings in the tunnel ceiling. No design response for that is offered here.

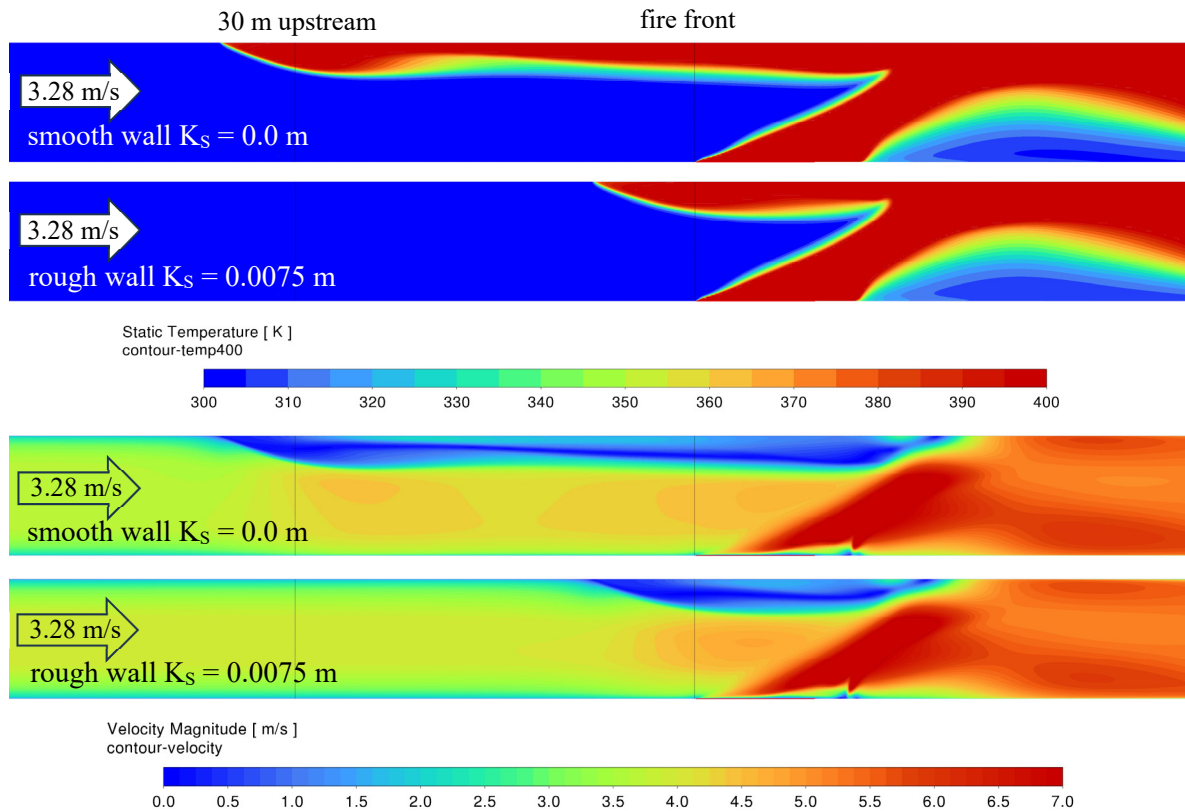


Figure 10: Contour plot of temperature (top) and velocity distribution (bottom) through the middle of the tunnel for confinement velocity with smooth wall and with increased wall roughness (5 times higher compared to initial case). Temperature is clipped to 400 K and velocity to 7 m/s for better presentation.

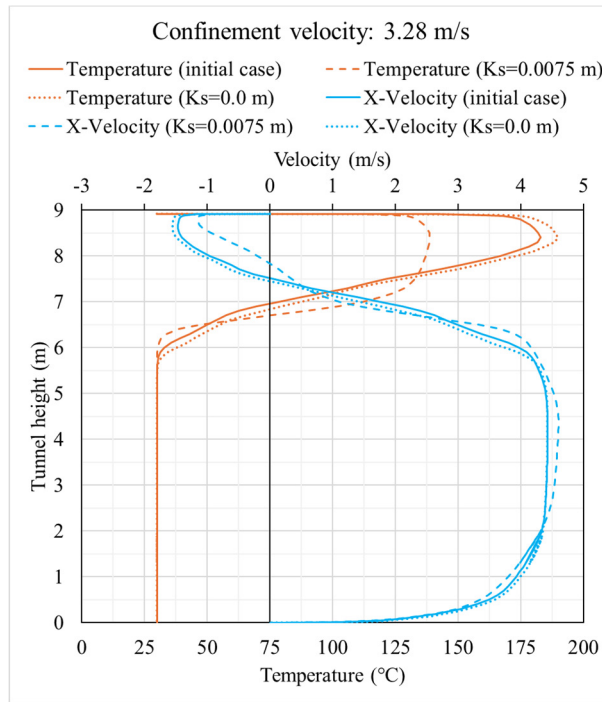
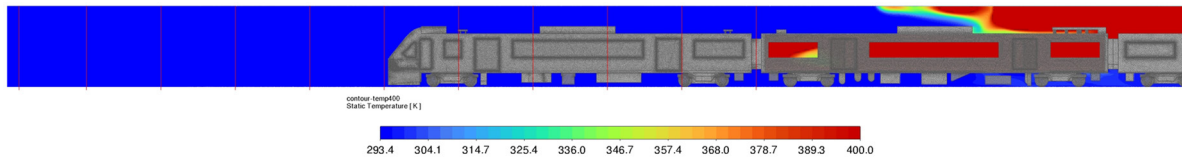


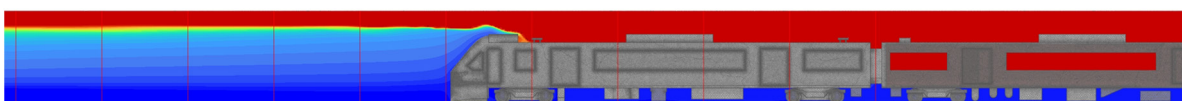
Figure 11: Velocity and temperature profile at the fire front for the initial case with confinement velocity and for the case with increased wall roughness. Profile was created on a vertical line from tunnel floor to ceiling in the symmetry plane of the tunnel profile.

Rail tunnel (high blockage ratio): Using a previously established model of a real case, the air velocity onto the fire was slightly decreased until smoke started propagating upstream. The train in the tunnel restricts the free flow area so that the annular air velocity over the train is higher (here 1.446 times higher) than the average velocity upstream of the train. Once smoke starts propagating upstream and passes the head of the train, the approaching air velocity is much lower and so the smoke starts spreading more readily upstream. Figure 12 illustrates the smoke propagation as the temperature distribution, for the case where upstream propagation of the smoke was just prevented (annular velocity of 1.8 m/s) and the case where smoke was propagating freely upstream (annular velocity of 1.7 m/s). Just a small change in the annular velocity (0.1 m/s) was enough for a change between controlled and uncontrolled conditions. That behaviour might be related to the low velocity values (approximately 1.2 m/s upstream of the train) and the associated low dynamic pressure (stagnation pressure). As soon as the buoyancy force overwhelms the inertia force, the resulting forces on the smoke backlayer are too small to stop their continued upstream propagation. At such low velocities, the mixing that cools the smoke shear layer and assists to blow it downstream, is much reduced.

Annular velocity: 1.8 m/s (1.25 m/s upstream)



Annular velocity: 1.7 m/s (1.18 m/s upstream)



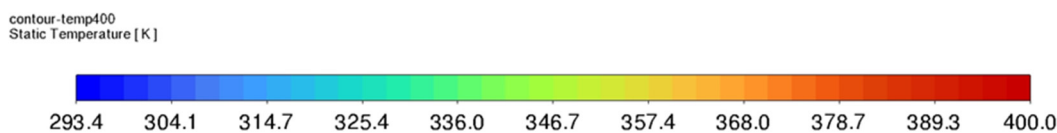


Figure 12: Contour plot of temperature through the middle of the tunnel (long section) for a 15 MW fire and an annular velocity of 1.8 m/s (top) and 1.7 m/s (bottom). Temperature is clipped to 400 K for better presentation. Grid marks (red lines) are at 5 m intervals.

4.4. Practical Approach for Estimating Confinement Velocity

If the typical wall roughness height of the concrete lining is not much less than assumed for the CFD investigation (see Table 1), then the influence due to wall roughness may be less relevant. Something similar can be concluded on the wall heating effect. If a typical fire scenario in a tunnel does not last longer than 30 to 60 minutes, the slow upstream propagation of the smoke backlayer due to the tunnel wall heating over time may still provide acceptable conditions during egress. For conservatism, a tunnel slope could be neglected. Based on that discussion and accepting some variation in the backlayer distance, equation (2) in combination with a modified Richardson number of 1.25 (see Section 4.3.1) could be used for a first guess of confinement velocity (backlayer distance of approximately 30 m). That assumes that the resulting confinement velocity is still sufficiently high (say >2.5 m/s but may need to be higher for sloped tunnels), that the neglected effects on the fire plume and backlayering dynamics do not drastically affect the balance of the counteracting forces and cause an upstream propagation of hot smoke without bounds (see discussion around Figure 12).

However, this proposal to use a modified Richardson number is based on a limited CFD study where a broader range of parameters was not systematically explored. It is not clear how a smaller tunnel area, a different tunnel shape, different tunnel height etc. affect the conclusions made for sloped tunnels. Further, the relationship between confinement and critical velocities may also be a function of the critical velocity. The lower the required critical velocity, the more unlikely it is that a smoke backlayer length can be controlled (kept stable). That also influences the sensitivity and variation of a backlayer length to wall roughness, wall heating etc. Finally, the sensitivities of backlayer distance as discussed in Section 4.3.1 have been explored based only on a 30 m long smoke backlayer. The conclusions made are likely to be different for longer backlayer distances (lower confinement velocity) especially if wall heating is considered.

For now, it seems that the only reliable guide for evaluating confinement velocity is to use a CFD method validated for critical velocity (as proposed in [21]), hoping that the additional physics involved in the backlayer doesn't compromise the CFD model too seriously when allowing significant backlayering.

There are two aspects that may demand adjustment to the proposed CFD model for analysing confinement velocity.

The first is related to thermal radiation between the backlayering smoke and the surroundings. Considering the thermal radiation in the computational domain would supersede the applied radiative fraction approach in the proposed CFD model [21] and thus require a re-validation of the critical velocity cases first. Solving the additional transport equations for thermal radiation would add model complexity and notably increase the computing time. As discussed in Section 4, the influence on the backlayering of the radiative heat loss is assumed to be minor. Including radiation would likely lead to a shorter backlayering distance. Adding the extra complexity just for a minor correction is not seen to be a practical approach.

The second aspect is related to wall heating adjacent to the backlayering and how it affects the backlayering length over time. The proposed model methodology for modelling critical

velocity [21] suggests a steady state solver with constant wall temperature. That seems to be an acceptable approach for analysing critical velocity but needs to be reconsidered for analysing confinement velocity for reasons discussed in Section 4.2.

To include heat flow into the concrete tunnel lining over time would require a transient simulation and drastically increase the computation time. As an alternative, the tunnel wall upstream of the fire could be changed to an adiabatic wall (no heat exchange) to add conservatism, but that would overestimate the required confinement velocity. To still have a reasonably accurate outcome, the smoke propagation can be analysed with a constant wall temperature (same as approaching air) first. After establishing a desired steady state backlayer distance, the simulation could be run again, with an adjusted wall temperature within the region of the upstream smoke layer adjacent to the wall, as described in Section 4.3.

5. COMMENTARY AND CONCLUSION

From a fire life safety perspective, it makes sense to reduce the tunnel air velocity onto the fire so far as is reasonably practicable [27] [28] to optimise conditions for egress. This approach has been common practice especially in Europe via the PIARC [29] and national standards [28], [27], [25] but is also acknowledged in the 2023 version of NFPA 502 [3]. Instead of having a fixed design velocity depending on ventilation system and traffic conditions as usually adopted in Europe [29], [28], [27], [25], NFPA 502 [3] permits a design velocity (confinement velocity) that controls upstream smoke propagation to within a limiting length (e.g. 30 m).

As there is no guidance on how to establish confinement velocity, the essential physics on smoke propagation and confinement velocity were re-visited. Based on the mixed convection model for estimating critical velocity for smoke control in road tunnels [17], the local fire plume dynamics relevant to establishing or preventing upstream smoke propagation were summarised. Once smoke is propagating upstream, additional parameters and effects become relevant. The most important parameters influencing the backlayer dynamics were discussed, and their influences on the backlayer distance explored by means of a CFD model validated for critical velocity. The outcomes of that study, based on the fire and tunnel characteristics investigated were that:

- For a typical high arched road tunnel, the difference between critical velocity and confinement velocity with a 30 m smoke backlayer was found to be approximately 7%.
- Confinement velocity is actually lower in downgrade tunnels. For the same airspeed confining smoke to 30 m upstream in a flat tunnel, backlayer distance was reduced by 50% for the 4% and 8% downgrade tunnels.
- The heat transfer from the upstream smoke layer to the tunnel wall increases the wall surface temperature over time which causes the smoke layer to slowly propagate upstream and increases the backlayer length by 18% over a period of 60 minutes.
- Compared to a typical tunnel wall roughness (roughness height of 0.0015 m), a smooth wall increased backlayer length by 19%. Backlayer length was reduced by 75% for a wall roughness that was 5 times higher than the typical value.
- Especially in highly blocked tunnels (e.g. rail tunnels), once critical velocity value is already very low (<2 m/s), confinement velocity is no different to critical velocity.

However, those outcomes are based on a limited CFD study, with only one fire scenario in each example tunnel. It is unclear how the effects that were explored might impact the upstream smoke propagation for different fire scenarios, tunnel geometries or different confinement velocity definitions (e.g. accepted backlayer length). For the time being, it is recommended to use a CFD model validated against critical velocity (as proposed in [21] and

discussed in this paper), with the hope that the additional physics involved in the backlayer are still captured well enough to not invalidate the outcome.

6. REFERENCES

- [1] P. Sturm, M. Beyer and M. Rafiei, "On the problem of ventilation control in case of a tunnel fire event," *Case Studies in Fire safety, CSFS 22, Elsevier publishing*, doi: 10.1016/j.csfs.2015.11.001, 2015.
- [2] M. Beyer, C. Stacey and A. Dix, "Critical velocity and tunnel smoke control Part 2, Filling the NFPA 502 void," *Australian Tunnelling Society*, p. 6, 2021.
- [3] NFPA 502, "Standard for Road Tunnels, Bridges, and Other Limited Access Highways," The National Fire Protection Association, US, 2023.
- [4] G. W. Kile and J. A. Gonzalez, "The Memorial Tunnel Fire Ventilation Test Program: The Longitudinal and Natural Tests," *ASHRAE Transactions 103, ProQuest Science Journals*, p. 701, 1997.
- [5] MTFVTP, "Memorial Tunnel Fire Ventilation Test Program - Comprehensive Test Report," Bechtel/Parsons Brinckerhoff, Boston, 1995a.
- [6] MTFVTP, "Memorial Tunnel Fire Ventilation Test Program - Memorial Tunnel Test Data Report incl. 9 discs of raw data," Bechtel/Parsons Brinckerhoff, Boston, 1995b.
- [7] D. Fruhwirt, P. Sturm, M. Bacher and H. Schwingenschlögl, "Smoke Propagation in Tunnels - Comparison of In-Situ Measurements, Simulations and Literature," in *10th International Conference "Tunnel Safety and Ventilation"*, Graz, 2020.
- [8] S. R. Lee and S. Ryou, "An Experimental Study of the Effect of the Aspect Ratio on the Critical Velocity in Longitudinal Ventilation Tunnel Fires," *Journal of Fire Sciences*, no. 23, pp. 119-138, 2005.
- [9] Y. Oka and G. T. Atkinson, "Control of Smoke Flow in Tunnel Fires," *Fire Safety Journal*, no. 25, pp. 305-322, 1995.
- [10] G. T. Atkinson and Y. Wu, "Smoke Control in Sloped Tunnels," *Fire Safety Journal*, no. 27, pp. 335-341, 1996.
- [11] Y. Wu and M. Z. A. Bakar, "Control of smoke flow in tunnel fires using longitudinal ventilation system – a study of the critical velocity," *Fire Safety Journal*, no. 35, pp. 363-390, 2000.
- [12] Y. Li and H. Ingason, "Study of critical velocity and backlayering length in longitudinally ventilated tunnel fires," *Fire Safety Journal*, no. 45, pp. 361-370, 2010.
- [13] Y. Li and H. Ingason, "Effect of cross section on critical velocity in longitudinally ventilated tunnel fires," *Fire Safety Journal*, no. 91, pp. 303-311, 2017.
- [14] Y. Li and H. Ingason, "Corrigendum to "Effect of cross section on critical velocity in longitudinally vent-lated tunnel fires" [Fire Saf. J. 91 (2017) 303-311]," *Fire Safety Journal*, no. 110, 2019.

- [15] Y. Li and H. Ingason, "Discussions on critical velocity and critical Froude number for smoke control in tunnels with longitudinal ventilation," *Fire Safety Journal*, no. 99, pp. 22-26, 2018.
- [16] C. Stacey and M. Beyer, "Critical of critical velocity - An industry practioner's perspective," in *10th International Conference 'Tunnel Safety and Ventilation'*, Graz, 2020a.
- [17] M. Beyer, C. Stacey and G. Brenn, "A Mixed Convection Model for Estimating the Critical Velocity to Prevent Smoke Backlayering in Tunnels," *Springer Fire Technology*, no. prepring, p. 50, 2024.
- [18] P. Thomas, "The Movement of Smoke in Horizontal Passages Against an Air Flow," *Fire Research Station*, no. Fire Research Note No 723, 1968.
- [19] P. Thomas, "The Movement of Buoyant Fluid Against a Stream and the Venting of Under-ground Fires," *Fire Research Station*, no. Fire Research Note No 351, 1958.
- [20] W. Kennedy, "Critical velocity: Past, Present and Future," *Seminar of Smoke and Critical Velocity in Tunnels*, pp. 305-322, 9-11 March 1996.
- [21] M. Beyer and C. Stacey, "CFD Validation for Tunnel Smoke Control Design," in *11th International Conference Tunnel Safety and Ventilation*, Graz, 9th and 10th May 2022.
- [22] Ansys, Inc, "ANSYS Fluent Theory Guide, Release January 2023 R2," USA, 2023b.
- [23] Ansys, Inc, "ANSYS Fluent User's Guide, Release January 2023 R2," USA, 2023a.
- [24] Ansys, Inc, "ANSYS Fluid Dynamics Verification Manual, Release January 2023 R2," USA, 2023c.
- [25] RABT, "Richtlinie für die Ausstattung und den Betrieb von Straßentunnel (RABT)," Richtlinie, Forschungsgesellschaft für Straßen- und Verkehrswesen , Arbeitsgruppe Verkehrsführung und Verkehrssicherheit, Germany, 2016.
- [26] J. Raposo, E. Cavaco, L. Neves and E. Julio, "A novel roughness parameter for more precise eztimation of the shear strength of concrete-to-concrete interfaces," *Elsevier ScienceDirect*, vol. 410, no. Construction and Building Materials 410, p. 12, 2024.
- [27] ASTRA, "Lüftung der Strassentunnel - Systemwahl, Dimensionierung und Ausstattung (2008 V2.03)," Richtlinie, Bundesamt für Strassen ASTRA, Bern, CH, 2008.
- [28] RVS 09.02.31, "Tunnel / Tunnel Equipment / Ventilation Systems - Basic Principles," Richtlinie, Österreichische Forschungsgesellschaft Straße - Schiene - Verkehr, Wien, AT, 2014.
- [29] PIARC (C3.3), "Operational Strategies for Emergency Ventilation (P. C. (C3.3), Ed.)," World Road Association (PIARC), 2011.